Analytical Investigations of the Mechanotransduction of Mesenchymal Stem Cell for Regulating Cell Fate Decisions

[1]Adeleye OA, [2]Omotosho-Dare T, [3]Yinusa AA

[1]Department of Biomedical Engineering, University of Lagos, Akoka, Lagos, Nigeria.
[2]Department of Systems Engineering, University of Lagos, Akoka, Lagos, Nigeria.
[3]Department of Mechanical Engineering, University of Lagos, Akoka, Lagos, Nigeria.

Corresponding Author
OA Adeleye
Department of Biomedical Engineering, University of Lagos, Akoka, Lagos, Nigeria.
Email: rotimiadeleye1711@gmail.com; Tel.: +234 805 522 5840

ABSTRACT

Background: The evolution of new biomaterials in tissue engineering is under constant investigation. These biomaterials undergo mechanical stimuli induced cell-differentiation of the mesenchymal stem cell in their transition stage, and the developed dynamic model for this mechanotransduction (mechanical stimuli) process for regulating the fate of the mesenchymal stem cell is a set of coupled nonlinear differential equations whose exact solutions cannot be easily obtained with the common analytical methods.

Objective: The analytical investigation of the dynamical model for the mechanotransduction of mesenchymal stem cell for regulating cell fate decisions is presented.

Methods: A special analytic technique known as Differential transform method (DTM) was applied to obtain the solutions for the developed dynamic model and was validated with the fourth order Runge-Kutta numerical method (RK4).

Results: The obtained analytical solutions have good agreement with the RK4 numerical solutions and past simulated studies. The effects of systems' large (30k–300k) and low (0k–1.0k) stiffness levels, k_1 and degradation rate of the corresponding gene factor d_1 on effective stiffness adhesion area were investigated. At low values of the system's high stiffness (30k–300k), the effective stiffness adhesion area reduces, and at large stiffness level, the curve becomes asymptotic, but when it is further increased, it has a negligible impact on the effective stiffness adhesion area. It is also observed that at low values of the system's low stiffness (0k–1.0k), the low stiffness k_1 and degradation rate of the corresponding gene factor d_1 shows a negligible impact on the effective stiffness adhesion area at the initial state of response, while an increase in the low stiffness k_1 causes a corresponding increase in effective stiffness adhesion area, but an increase in degradation rate factor d_1 causes a decrease in effective stiffness adhesion area.

Conclusion: The obtained results from the dynamical analysis can be applied in developing new techniques in controlling the fate of mesenchymal stem cell's transplantation and designs of new biomaterials.

Keywords: Mesenchymal stem cell, Cell fate decision, Nonlinear dynamics, Mathematical modeling, Differential transform method.

INTRODUCTION

The evolution of new biomaterials in tissue engineering is under constant investigation. Explicitly, there is a growing interest for the usage of designed biomaterials in the field of stem cell study and applications, because biomaterials can be utilized in manipulating the cell reactions thereby providing a control of the behaviour of these biomaterials (1). This is of great significance because of the ability to engineer complexities and also latter *in vitro* growth of tissues and organs, which remains a key objective for tissue engineers. Biomaterials are either natural or synthetic matrices that can be used to provide suitable microenvironment for cell growth and differentiation, in restoring the function and structure of body tissue (2). Biomaterials adopted for engineering organs and tissues can be categorized into three groups; naturally gotten materials, synthetic polymers and tissue matrices. Natural polymers include the likes of collagen, keratin and alginate which can be sourced autologously, allogenically from others or xenogenically from other species. Synthetic polymers such as polyglycolic acid (PGA) and polylactic acid (PLA) undergo polymerization to form poly (-lactic-co-glycolic) acid which is then used to in scaffold fabrication. Tissue matrices involves decellularization of cells which then proceeds to the addition of glycosaminoglycans(GAGs) to form seeded cells which marks the recellularization process (3).

Mesenchymal stem cells are non-specialized cells with the ability to differentiate (become other cell types) (1), and this process of differentiation is usually determined by past memory of external mechanical stimuli, the effect of mechanotransduction has proven that cells can sense and incorporate mechanical signals perceived from the extracellular matrix of the body(4). There are different modes of mechanotransduction such as direct and indirect mechanotransduction (5). Mathematical models of

mechanotransduction have been developed to best describe cell differentiation as instructed by external mechanical signals. A potent illustration involves the analysis of the role of Yes-associated protein/ Transcriptional coactivator (YAP/TAZ) in mechanosensing (6).

An understanding the effect of mechanical memory in mesenchymal stem cell differentiation into cell fates helps in the engineering of stem cells in tissue regenerative biomaterials for therapeutic purposes (7). Biomaterials are being applied in increasingly complex areas such as tissue engineering, regenerative procedures, and more recently bio printing (8). Biomaterials when introduced to the human body are inherently dynamic, they are biocompatibly engineered to be capable of sensing mechanical cues from their surrounding environments and produce the appropriate responsive signal (9). Some dynamic characteristics of biomaterials include; self-organization, mechanochemical responsiveness and self-healing. Self-organization describes the spontaneous congregation of the elements of the biomaterial without the intervention of any external forces (10). The mechanochemical responsiveness deals with the biocompatibility of the biomaterial and the body which depends on various chemical and physical conditions of the various environments (11). And the self-healing demonstrates the ability of an engineered biomaterial to induce a physiological response that supports the function and performance of the biomaterial (8).

The extracellular matrix (ECM) in living organisms is made up of micro and Nano scaled topographical features that relate with cells behaviour and thus provides the bases to develop artificial architectures that will induce the differentiation of cell by stem cells and surfaces interaction (12). The extracellular matrix provides an anchor for the biomaterials to ligate with in most mammalian cell. In order to simulate the relationship of cells with the extracellular matrix, focal adhesion is formed through Ligand-occupied integrin (13). Focal adhesions act as an internal scaffold and generally their size is dependent on the total number of actin fibers the integrin is able to gather together.

Stem cells are undifferentiated cells which have the ability to differentiate into multiple cell types (multipotency) and also to self-renew (14). Because of this ability of multipotency, they offer great promise in the field of regenerative medicine because the regeneration of organs depends on tissues which in turn depend essentially on the ability of stem cells to differentiate into particular cell types (15). Since Tissue Engineering (TE) and organ regeneration focus on the use of biomaterials to regenerate damaged tissue and or certain organs of the human body, precise control over the differentiation and ultimate fate of the stem cell becomes imperative to the development of such therapeutic strategies (16). Biophysical cues play vital roles in regulating cellular behaviour both *in vivo* and *in vitro*, also studies have shown that the fate of a stem cell depends on a number of factors viz a viz: stiffness (elasticity and topography of the extracellular matrix. Noticeable changes in the conditions of the cell can be coordinated by mechanical cues from the surrounding microenvironment of the cell, for example, the local extracellular matrix stiffness. In recent study, it has been established in mechanotransduction that cells receive and incorporate mechanical signals from the extracellular matrix (ECM), which causes transcriptional changes to happen and ultimately affect cell fate decisions (7). To relate effectively with the ECM, cells adopt the use of receptors such as integrin that binds itself to specific peptide motifs within the ECM (17).

Stem cells play distinctive role, adequately meet the requirement of the complexity in TE and demand accurate organization of directive signals all through a cell scaffold. These imply producing man-made dummies that emulate the key attributes of extracellular matrix (ECM) (18). When developing biomaterials, the first obstacle to address would be that of adhesion with the stem cells. Stem cells are anchorage-dependent and hence must adhere to the substrate for survival (19). In the development of biomaterials over the years, there is a movement toward the biomaterial production where the control of cell by reproducible molecular is initiated, and the tissue regeneration genome are activated (20). Hence the Mesenchymal stem cells (MSCs) are directed by cues from the ECM and the gene expression patterns differential is wide (21).

The fate of Mesenchymal stem cell (MSC) could be determined by mechanical memory (which can be from past dosing) through the stem cell differentiation. This has great effects on the stem cell fate especially when its initial substrate has high stiffness. This is nonetheless tedious to experimentally put to test over a wide range of culture conditions. However, a mathematical model has been developed for the prediction of the fates of the mesenchymal stem cells through the dynamics of mechanical dosing (memory) of the mesenchymal stem cells. This provides a predictive model for the experimental data (22). The developed model is analysed over long period of time to determine the mechanical memory region which exists for all of the MSC-derived cell differentiations and the model is a gene regulatory precise network that determines MSC fate and it is represented by a set of nonlinear ordinary differential equations (ODEs).

The dynamic model in this investigation is a set of nonlinear ordinary differential equations whose closed form solution does not exist, hence, it solved by applying Differential transform method (DTM). The Differential Transform Method (DTM) is a semi-analytical method for solving linear and highly non-linear differential equations developed by Zhou (23). It is efficient in solving flow problems as observed in squeezing flow of cu-water and cu-kerosene nanofluids between two parallel plates (24). It is also efficient in providing solutions to Newtonian and non-Newtonian nanofluids flow analysis (25). In addition it is also effective in handling fin problems with internal heat generation and temperature-dependent properties (26) and nonlinear ordinary differential matrix equations (27). The DTM has also been compared with Homotopy Perturbation Method (HPM) for a System of Non Linear Chemistry Problems (28) and The Adomian Decomposition Method (ADM) (29) and has proved to be effective. The deficiency of slowed convergence in DTM can be overcome by combining it with Laplace transform as shown in Approximate solution for nonlinear Duffing oscillator with damping effect using the modified differential transform method (30) and the Application of the fractional differential transform method to fractional-order integro-

differential equations has proved effective in overcoming fractional-order (31).

Hence, the aim of this study is to develop an analytical tool for the prediction of the fates of the mesenchymal stem cells through the dynamics of mechanical dosing (memory) of the mesenchymal stem cells in tissue regenerative biomaterials. Hence, a nonlinear dynamical model of the mechano-transduction of mesenchymal stem cell that is able to describe the cell fate transitions that occur during mechanical stimuli directed cell-differentiation is developed. The developed dynamic model is a set of coupled nonlinear differential equations which cannot be solved by the common analytical techniques. It is then solved by applying Differential transform method (DTM) and verified using the forth order Runge-Kutta numerical method (RK4). The effects of systems' large (30k-300k) and low (0k-1.0k) stiffness levels, k_1 and degradation rate of the corresponding gene factor d_1 on the effective stiffness adhesion area are then investigated.

Problem Description and Formulation of Equation

The mechanical memory exhibited by the mesenchymal stem cells can be illustrated as shown in Figure 1 *(a, b, c, d)* as developed by Peng *et al.* (7). These MSCs are differentiated into specific path under various substrate stiffness states by the gene encoded Tubulin beta-3chain *TUBB3 (T)*. However, for long first seeding durations which is usually more than 10 days, the past mechanical memory of the external stimuli results into heterogeneous osteogenic differentiation (Figure 1) *(g, h)*.

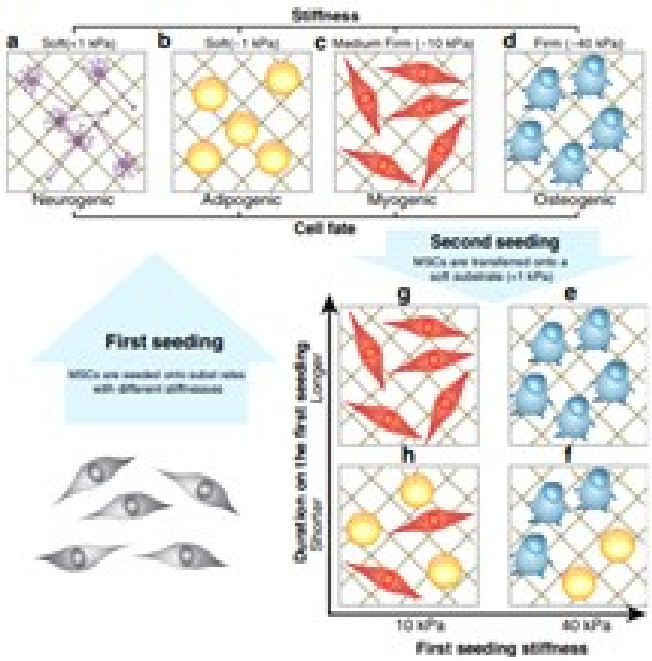

Fig. 1: Cell Unit Degree of Freedom.

For the purpose of deriving a model for these predictions, a regulatory network is applied in developing the mathematical model (Figure 2).

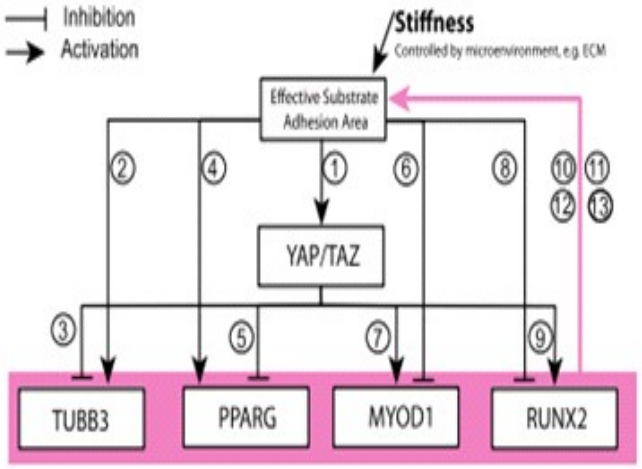

Fig. 2: The Regulatory Network used for Modelling.

The potential function is projected into two-dimensional plane for visualization, which are the model species *(YAP/TAZ)*, and the effective stiffness adhesion area *(SAA)*. Hence, the four remaining system variables *(TUBB3, PPARG, MYOD1, and RUNX2)* are integrated. The system's variables are represented as shown in Table 1.

Table 1: System's Variables and Representation

S/N	Variables	Representation
1	YAPTAZ	Y
2	SAA	S
3	TUBB3	T
4	PPARG	P
5	MYOD1	M
6	RUNX2	R

Considering the dynamic response of mesenchymal stem cell fate and the representation (Table 1), a simplified network model for gene regulation in *MSC* fate decision is developed into the following sets of nonlinear ordinary differential equations:

$$\frac{dS(t)}{dt} - k_1\left(\left(\frac{X}{K_1}\right)^{n_1} + \left(\frac{T(t)}{K_2}\right)^{n_2}\right)\left(1+\left(\frac{X}{K_1}\right)^{n_1} + \left(\frac{T(t)}{K_2}\right)^{n_2}\right)^{-1} -$$
$$k_2\left(\left(\frac{X}{K_3}\right)^{n_3} + \left(\frac{P(t)}{K_4}\right)^{n_4}\right)\left(1+\left(\frac{X}{K_3}\right)^{n_3} + \left(\frac{P(t)}{K_4}\right)^{n_4}\right)^{-1} \quad (1)$$
$$-k_3\left(\left(\frac{X}{K_5}\right)^{n_5} + \left(\frac{M(t)}{K_6}\right)^{n_6}\right)\left(1+\left(\frac{X}{K_5}\right)^{n_5} + \left(\frac{M(t)}{K_6}\right)^{n_6}\right)^{-1} -$$
$$k_4\left(\left(\frac{X}{K_7}\right)^{n_7} + \left(\frac{R(t)}{K_8}\right)^{n_8}\right)\left(1+\left(\frac{X}{K_7}\right)^{n_7} + \left(\frac{R(t)}{K_8}\right)^{n_8}\right)^{-1} + d_1 S(t) = 0$$

$$\frac{dY(t)}{dt} - k_5 S(t) + d_2 Y(t) = 0 \tag{2}$$

$$\frac{dT(t)}{dt} - k_6 \left(\frac{S(t)}{K_9}\right)^{n_9} \left(1 + \left(\frac{S(t)}{K_9}\right)^{n_9} + \left(\frac{Y(t)}{K_{10}}\right)^{n_{10}}\right)^{-1} + d_3 T(t) = 0 \tag{3}$$

$$\frac{dP(t)}{dt} - k_7 \left(\frac{S(t)}{K_{11}}\right)^{n_{11}} \left(1 + \left(\frac{S(t)}{K_{11}}\right)^{n_{11}} + \left(\frac{Y(t)}{K_{12}}\right)^{n_{12}}\right)^{-1} + d_4 P(t) = 0 \tag{4}$$

$$\frac{dM(t)}{dt} - k_8 \left(\frac{Y(t)}{K_{13}}\right)^{n_{13}} \left(1 + \left(\frac{S(t)}{K_{14}}\right)^{n_{14}} + \left(\frac{Y(t)}{K_{13}}\right)^{n_{13}}\right)^{-1} + d_5 M(t) = 0 \tag{5}$$

$$\frac{dR(t)}{dt} - k_9 \left(\frac{Y(t)}{K_{15}}\right)^{n_{15}} \left(1 + \left(\frac{S(t)}{K_{16}}\right)^{n_{16}} + \left(\frac{Y(t)}{K_{15}}\right)^{n_{15}}\right)^{-1} + d_6 R(t) = 0 \tag{6}$$

Where *di* (i = 1, 2,…, 6) in Eqs. (1–6) are the corresponding factors for rates of gene degradation, and the *Ki* (i = 1, 2,…, 9) the stiffness of the system.

The nonlinear model is coupled with initial conditions expressed as:

$$\begin{aligned} S(0) &= S_0 = 0, \\ Y(0) &= Y_0 = 0, \\ T(0) &= T_0 = 0, \\ P(0) &= P_0 = 0, \\ M(0) &= M_0 = 0, \\ R(0) &= R_0 = 0. \end{aligned} \tag{7}$$

In the established equations (1–6), the dependent variables are in index form. Their presence as denominators also makes it complex to develop exact solutions. However, since it is in the interest of this research to develop analytical solutions to the system of coupled ODEs in order to enhance parametric studies, Differential transform method (DTM) by representation will be employed.

Representing the Complex Dependent Variables in the Model

For the complex term representation, the approach is illustrated below:

$$\text{Let} \quad \begin{aligned} f_2 &= T^{n_2} \\ f_4 &= P^{n_4} \\ f_6 &= M^{n_6} \\ f_8 &= R^{n_8} \\ f_9 &= S^{n_9} \\ f_{10} &= Y^{n_{10}} \end{aligned} \quad \text{and} \quad \begin{aligned} f_{11} &= S^{n_{11}} \\ f_{12} &= Y^{n_{12}} \\ f_{13} &= Y^{n_{13}} \\ f_{14} &= S^{n_{14}} \\ f_{15} &= Y^{n_{15}} \\ f_{16} &= S^{n_{16}} \end{aligned} \tag{8}$$

$$\frac{df_2}{dt} = \frac{df_2}{dT}\frac{dT}{dt} = n_2 T^{n_2 - 1}\frac{dT}{dt}$$

$$\frac{df_2}{dt} = n_2 \frac{T^{n_2}}{T}\frac{dT}{dt} = \frac{n_2 T^{n_2}\dfrac{dT}{dt}}{T} = \frac{n_2 f_2 \dfrac{dT}{dt}}{T}$$

$$T\frac{df_2}{dt} - n_2 f_2 \frac{dT}{dt} = 0 \tag{9}$$

Similarly for the remaining dependent variables, the obtained differential equations are:

$$P\frac{df_4}{dt} - n_4 f_4 \frac{dP}{dt} = 0 \tag{10}$$

$$M\frac{df_6}{dt} - n_6 f_6 \frac{dM}{dt} = 0 \tag{11}$$

$$R\frac{df_8}{dt} - n_8 f_8 \frac{dR}{dt} = 0 \tag{12}$$

$$S\frac{df_9}{dt} - n_9 f_9 \frac{dS}{dt} = 0 \tag{13}$$

$$Y\frac{df_{10}}{dt} - n_{10} f_{10} \frac{dY}{dt} = 0 \tag{14}$$

$$S\frac{df_{11}}{dt} - n_{11} f_{11} \frac{dS}{dt} = 0 \tag{15}$$

$$Y\frac{df_{12}}{dt} - n_{12} f_{12} \frac{dY}{dt} = 0 \tag{16}$$

$$Y\frac{df_{13}}{dt} - n_{13} f_{13} \frac{dY}{dt} = 0 \tag{17}$$

$$S\frac{df_{14}}{dt} - n_{14} f_{14} \frac{dS}{dt} = 0 \tag{18}$$

$$Y\frac{df_{15}}{dt} - n_{15} f_{15} \frac{dY}{dt} = 0 \tag{19}$$

$$S\frac{df_{16}}{dt} - n_{16} f_{16} \frac{dS}{dt} = 0 \tag{20}$$

Substituting equation (8) into equations (1–6), we have:

$$\begin{aligned} &\frac{dS(t)}{dt} - k_1 \left(\left(\frac{X}{K_1}\right)^{n_1} + \left(\frac{1}{K_2}\right)^{n_2} f_2\right)\left(1 + \left(\frac{X}{K_1}\right)^{n_1} + \left(\frac{1}{K_2}\right)^{n_2} f_2\right)^{-1} - \\ &k_2 \left(\left(\frac{X}{K_3}\right)^{n_3} + \left(\frac{1}{K_4}\right)^{n_4} f_4\right)\left(1 + \left(\frac{X}{K_3}\right)^{n_3} + \left(\frac{1}{K_4}\right)^{n_4} f_4\right)^{-1} \\ &-k_3 \left(\left(\frac{X}{K_5}\right)^{n_5} + \left(\frac{1}{K_6}\right)^{n_6} f_6\right)\left(1 + \left(\frac{X}{K_5}\right)^{n_5} + \left(\frac{1}{K_6}\right)^{n_6} f_6\right)^{-1} - \\ &k_4 \left(\left(\frac{X}{K_7}\right)^{n_7} + \left(\frac{1}{K_8}\right)^{n_8} f_8\right)\left(1 + \left(\frac{X}{K_7}\right)^{n_7} + \left(\frac{1}{K_8}\right)^{n_8} f_8\right)^{-1} + d_1 S(t) = 0 \end{aligned} \tag{21}$$

$$\frac{dY(t)}{dt} - k_5 S(t) + d_2 Y(t) = 0 \tag{22}$$

$$\frac{dT(t)}{dt} - k_6\left(\frac{1}{K_9}\right)^{n_9} f_9\left(1+\left(\frac{1}{K_9}\right)^{n_9} f_9 + \left(\frac{1}{K_{10}}\right)^{n_{10}} f_{10}\right)^{-1} + d_3 T(t) = 0 \tag{23}$$

$$\frac{dP(t)}{dt} - k_7\left(\frac{1}{K_{11}}\right)^{n_{11}} f_{11}\left(1+\left(\frac{1}{K_{11}}\right)^{n_{11}} f_{11} + \left(\frac{1}{K_{12}}\right)^{n_{12}} f_{12}\right)^{-1} + d_4 P(t) = 0 \tag{24}$$

$$\frac{dM(t)}{dt} - k_8\left(\frac{1}{K_{13}}\right)^{n_{13}} f_{13}\left(1+\left(\frac{1}{K_{14}}\right)^{n_{14}} f_{14} + \left(\frac{1}{K_{13}}\right)^{n_{13}} f_{13}\right)^{-1} + d_5 M(t) = 0 \tag{25}$$

$$\frac{dR(t)}{dt} - k_9\left(\frac{1}{K_{15}}\right)^{n_{15}} f_{15}\left(1+\left(\frac{1}{K_{16}}\right)^{n_{16}} f_{16} + \left(\frac{1}{K_{15}}\right)^{n_{15}} f_{15}\right)^{-1} + d_6 R(t) = 0 \tag{26}$$

Which on simplifying yields:

$$\left(\begin{array}{l}\left(1+\left(\frac{X}{K_1}\right)^{n_1}+\left(K_2^{-1}\right)^{n_2} f_2\right)\left(1+\left(\frac{X}{K_3}\right)^{n_3}+\left(K_4^{-1}\right)^{n_4} f_4\right)\left(1+\left(\frac{X}{K_5}\right)^{n_5}+\left(K_6^{-1}\right)^{n_6} f_6\right)\left(1+\left(\frac{X}{K_7}\right)^{n_7}+\left(K_8^{-1}\right)^{n_8} f_8\right)\mathrm{D}(S)(t) - \\ k_1\left(\left(\frac{X}{K_1}\right)^{n_1}+\left(K_2^{-1}\right)^{n_2} f_2\right) - k_2\left(\left(\frac{X}{K_3}\right)^{n_3}+\left(K_4^{-1}\right)^{n_4} f_4\right) - k_3\left(\left(\frac{X}{K_5}\right)^{n_5}+\left(K_6^{-1}\right)^{n_6} f_6\right) - k_4\left(\left(\frac{X}{K_7}\right)^{n_7}+\left(K_8^{-1}\right)^{n_8} f_8\right) + \\ d_1\left(1+\left(\frac{X}{K_1}\right)^{n_1}+\left(K_2^{-1}\right)^{n_2} f_2\right)\left(1+\left(\frac{X}{K_3}\right)^{n_3}+\left(K_4^{-1}\right)^{n_4} f_4\right)\left(1+\left(\frac{X}{K_5}\right)^{n_5}+\left(K_6^{-1}\right)^{n_6} f_6\right)\left(1+\left(\frac{X}{K_7}\right)^{n_7}+\left(K_8^{-1}\right)^{n_8} f_8\right)S(t)\end{array}\right) = 0$$

Further simplification gives:

$$\left(\begin{array}{l}\mathrm{D}(S)(t) - \left(\frac{X}{K_1}\right)^{n_1} k_1 + k_1\left(\left(\frac{X}{K_1}\right)^{n_1}\right)^2 + 2\left(K_2^{-1}\right)^{n_2}\left(\frac{X}{K_1}\right)^{n_1} f_2 k_1 - \left(K_2^{-1}\right)^{n_2} f_2 k_1 + \\ k_1\left(\left(K_2^{-1}\right)^{n_2}\right)^2 f_2^2 - \left(\frac{X}{K_3}\right)^{n_3} k_2 + k_2\left(\left(\frac{X}{K_3}\right)^{n_3}\right)^2 + 2\left(\frac{X}{K_3}\right)^{n_3}\left(K_4^{-1}\right)^{n_4} f_4 k_2 - \\ \left(K_4^{-1}\right)^{n_4} f_4 k_2 + k_2\left(\left(K_4^{-1}\right)^{n_4}\right)^2 f_4^2 - \left(\frac{X}{K_5}\right)^{n_5} k_3 + k_3\left(\left(\frac{X}{K_5}\right)^{n_5}\right)^2 + \\ 2\left(K_6^{-1}\right)^{n_6}\left(\frac{X}{K_5}\right)^{n_5} f_6 k_3 - \left(K_6^{-1}\right)^{n_6} f_6 k_3 + k_3\left(\left(K_6^{-1}\right)^{n_6}\right)^2 f_6^2 - \left(\frac{X}{K_7}\right)^{n_7} k_4 + \\ k_4\left(\left(\frac{X}{K_7}\right)^{n_7}\right)^2 + 2\left(K_8^{-1}\right)^{n_8}\left(\frac{X}{K_7}\right)^{n_7} f_8 k_4 - \left(K_8^{-1}\right)^{n_8} f_8 k_4 + k_4\left(\left(K_8^{-1}\right)^{n_8}\right)^2 f_8^2 + d_1 S(t)\end{array}\right) = 0 \tag{27}$$

$$\frac{dY(t)}{dt} - k_5 S(t) + d_2 Y(t) = 0 \tag{28}$$

$$\left(1+\left(K_9^{-1}\right)^{n_9} f_9 + \left(K_{10}^{-1}\right)^{n_{10}} f_{10}\right)\frac{dT(t)}{dt} - k_6\left(K_9^{-1}\right)^{n_9} f_9 + d_3\left(1+\left(K_9^{-1}\right)^{n_9} f_9 + \left(K_{10}^{-1}\right)^{n_{10}} f_{10}\right)T(t) = 0 \tag{29}$$

$$\left(1+\left(K_{11}^{-1}\right)^{n_{11}} f_{11} + \left(K_{12}^{-1}\right)^{n_{12}} f_{12}\right)\frac{dP(t)}{dt} - k_7\left(K_{11}^{-1}\right)^{n_{11}} f_{11} + d_4\left(1+\left(K_{11}^{-1}\right)^{n_{11}} f_{11} + \left(K_{12}^{-1}\right)^{n_{12}} f_{12}\right)P(t) = 0 \tag{30}$$

$$\left(1+\left(K_{14}^{-1}\right)^{n_{14}} f_{14} + \left(K_{13}^{-1}\right)^{n_{13}} f_{13}\right)\frac{dM(t)}{dt} - k_8\left(K_{13}^{-1}\right)^{n_{13}} f_{13} + d_5\left(1+\left(K_{14}^{-1}\right)^{n_{14}} f_{14} + \left(K_{13}^{-1}\right)^{n_{13}} f_{13}\right)M(t) = 0 \tag{31}$$

$$\left(1+\left(K_{16}^{-1}\right)^{n_{16}} f_{16} + \left(K_{15}^{-1}\right)^{n_{15}} f_{15}\right)\frac{dR(t)}{dt} - k_9\left(K_{15}^{-1}\right)^{n_{15}} f_{15} + d_6\left(1+\left(K_{16}^{-1}\right)^{n_{16}} f_{16} + \left(K_{15}^{-1}\right)^{n_{15}} f_{15}\right)R(t) = 0 \tag{32}$$

Equations (27–32) together with equations (9–20) are resulting system of ODEs after representation. This ODEs will be solved analytically using the differential transform method (DTM) and after treatment will be applied where necessary.

Analytical Solution to the Developed Models

Basic Concept of Differential Transform Method (DTM)

Due to the presence of a nonlinearity in the derived coupled governing equation of motion, a method capable of transforming differential equations into another domain with a robust and easy way of inversion is required. Differential transform method (DTM) possesses this attribute. DTM maps a governing equation into an algebraic domain and then obtain an inversion using a series summation method. This approximate analytical method generates solution with the controlling parameters adequately conserved. The DTM recursive relation for transforming differential equation is shown in the illustration below:

$$Z(t) = U(t) \pm V(t), \quad Z(k) = U(k) \pm V(k).$$

$$Z(t) = \propto U(t), \quad Z(k) = \propto U(k).$$

$$Z(t) = \frac{dU(t)}{dt}, \quad Z(k) = (k+1)U[k+1].$$

$$Z(t) = \frac{d^2U(t)}{dt^2}, \quad Z(k) = (k+1)(k+2)U[k+2].$$

$$Z(t) = \frac{d^mU(t)}{dt^m}, \quad Z(k) = (k+1)(k+2)\cdots(k+m)U[k+m]. \quad \text{or} \frac{(k+m)!}{k!}U[k+m].$$

$$Z(t) = U(t) * V(t), \quad Z(k) = \sum_{l=0}^{K} V[l]\mathrm{U}[\mathrm{K}-l].$$

$$Z(t) = t^m, \quad Z(k) = \delta(k-m) = \begin{cases} 1 & if\ k = m \\ 0 & if\ k \neq m \end{cases}$$

Applying the DTM illustration to equations (9–20) together with equations (27–32) yield:

$$(\Gamma)(k+1)f_{2k+1} + \sum_{l=0}^{k} T_l(k+1-l)f_{2k+1-l} - n_2\sum_{l=0}^{k} f_{2l}(k+1-l)T_{k+1-l} = 0 \tag{33}$$

$$(\Gamma)(k+1)f_{4k+1} + \sum_{l=0}^{k} P_l(k+1-l)f_{4k+1-l} - n_4\sum_{l=0}^{k} f_{4l}(k+1-l)P_{k+1-l} = 0 \tag{34}$$

$$(\Gamma)(k+1)f_{6k+1} + \sum_{l=0}^{k} M_l(k+1-l)f_{6k+1-l} - n_6\sum_{l=0}^{k} f_{6l}(k+1-l)M_{k+1-l} = 0 \tag{35}$$

$$(\Gamma)(k+1)f_{8k+1} + \sum_{l=0}^{k} R_l(k+1-l)f_{8k+1-l} - n_8\sum_{l=0}^{k} f_{8l}(k+1-l)R_{k+1-l} = 0 \tag{36}$$

$$(\Gamma)(k+1)f_{9k+1} + \sum_{l=0}^{k} S_l(k+1-l)f_{9k+1-l} - n_9\sum_{l=0}^{k} f_{9l}(k+1-l)S_{k+1-l} = 0 \tag{37}$$

$$(\Gamma)(k+1)f_{10k+1} + \sum_{l=0}^{k} Y_l(k+1-l)f_{10k+1-l} - n_{10}\sum_{l=0}^{k} f_{10l}(k+1-l)Y_{k+1-l} = 0 \tag{38}$$

$$(\Gamma)(k+1)f_{11k+1} + \sum_{l=0}^{k} S_l(k+1-l)f_{11k+1-l} - n_{11}\sum_{l=0}^{k} f_{11l}(k+1-l)S_{k+1-l} = 0 \tag{39}$$

$$(\Gamma)(k+1)f_{12k+1} + \sum_{l=0}^{k} Y_l(k+1-l)f_{12k+1-l} - n_{12}\sum_{l=0}^{k} f_{12l}(k+1-l)Y_{k+1-l} = 0 \tag{40}$$

$$(\Gamma)(k+1)f_{13k+1} + \sum_{l=0}^{k} Y_l(k+1-l)f_{13k+1-l} - n_{13}\sum_{l=0}^{k} f_{13l}(k+1-l)Y_{k+1-l} = 0 \tag{41}$$

$$(\Gamma)(k+1)f_{14k+1} + \sum_{l=0}^{k} S_l(k+1-l)f_{14k+1-l} - n_{14}\sum_{l=0}^{k} f_{14l}(k+1-l)S_{k+1-l} = 0 \tag{42}$$

$$(\Gamma)(k+1)f_{15k+1} + \sum_{l=0}^{k} Y_l(k+1-l)f_{15k+1-l} - n_{15}\sum_{l=0}^{k} f_{15l}(k+1-l)Y_{k+1-l} = 0 \tag{43}$$

$$(\Gamma)(k+1)f_{16k+1} + \sum_{l=0}^{k} S_l(k+1-l)f_{16k+1-l} - n_{16}\sum_{l=0}^{k} f_{16l}(k+1-l)S_{k+1-l} = 0 \tag{44}$$

$$
\begin{pmatrix}
(k+1)S_{k+1}+\begin{pmatrix}
k_1\left(\left(\frac{X}{K_1}\right)^{n_1}\right)^2-\left(\frac{X}{K_1}\right)^{n_1}k_1-\left(\frac{X}{K_3}\right)^{n_3}k_2+\\
k_2\left(\left(\frac{X}{K_3}\right)^{n_3}\right)^2-\left(\frac{X}{K_5}\right)^{n_5}k_3+k_3\left(\left(\frac{X}{K_5}\right)^{n_5}\right)^2-\\
\left(\frac{X}{K_7}\right)^{n_7}k_4+k_4\left(\left(\frac{X}{K_7}\right)^{n_7}\right)^2
\end{pmatrix}\delta(k)+\\
2\left(K_2^{-1}\right)^{n_2}\left(\frac{X}{K_1}\right)^{n_1}k_1f_{2k}-\left(K_2^{-1}\right)^{n_2}k_1f_{2k}+\\
k_1\left(\left(K_2^{-1}\right)^{n_2}\right)^2\sum_{l=0}^{k}f_{2l}f_{2k-l}+2\left(\frac{X}{K_3}\right)^{n_3}\left(K_4^{-1}\right)^{n_4}k_2f_{4k}-\\
\left(K_4^{-1}\right)^{n_4}k_2f_{4k}+k_2\left(\left(K_4^{-1}\right)^{n_4}\right)^2\sum_{l=0}^{k}f_{4l}f_{4k-l}+\\
2\left(K_6^{-1}\right)^{n_6}\left(\frac{X}{K_5}\right)^{n_5}f_{6k}k_3-\left(K_6^{-1}\right)^{n_6}f_{6k}k_3+\\
k_3\left(\left(K_6^{-1}\right)^{n_6}\right)^2\sum_{l=0}^{k}f_{6l}f_{6k-l}+2\left(K_8^{-1}\right)^{n_8}\left(\frac{X}{K_7}\right)^{n_7}f_{8k}k_4-\\
\left(K_8^{-1}\right)^{n_8}f_{8k}k_4+k_4\left(\left(K_8^{-1}\right)^{n_8}\right)^2\sum_{l=0}^{k}f_{8l}f_{8k-l}+d_1S_k
\end{pmatrix}=0 \quad (45)
$$

$$
(k+1)Y_{k+1}-k_5S_k+d_2Y_k=0 \quad (46)
$$

$$
(k+1)T_{k+1}+\left(K_9^{-1}\right)^{n_9}\sum_{l=0}^{k}(l+1)T_{l+1}f_{9k-l}+\left(K_{10}^{-1}\right)^{n_{10}}\sum_{l=0}^{k}(l+1)T_{l+1}f_{10k-l}-k_6\left(K_9^{-1}\right)^{n_9}f_{9k}+
d_3\left(T_k+\left(K_9^{-1}\right)^{n_9}\sum_{l=0}^{k}T_lf_{9k-l}+\left(K_{10}^{-1}\right)^{n_{10}}\sum_{l=0}^{k}T_lf_{10k-l}\right)=0 \quad (47)
$$

$$
(k+1)P_{k+1}+\left(K_{11}^{-1}\right)^{n_{11}}\sum_{l=0}^{k}(l+1)P_{l+1}f_{11k-l}+\left(K_{12}^{-1}\right)^{n_{12}}\sum_{l=0}^{k}(l+1)P_{l+1}f_{12k-l}-
k_7\left(K_{11}^{-1}\right)^{n_{11}}f_{11k}+d_4\left(P_k+\left(K_{11}^{-1}\right)^{n_{11}}\sum_{l=0}^{k}P_lf_{11k-l}+\left(K_{12}^{-1}\right)^{n_{12}}\sum_{l=0}^{k}P_lf_{12k-l}\right)=0 \quad (48)
$$

$$
(k+1)M_{k+1}+\left(K_{14}^{-1}\right)^{n_{14}}\sum_{l=0}^{k}(l+1)M_{l+1}f_{14k-l}+\left(K_{13}^{-1}\right)^{n_{13}}\sum_{l=0}^{k}(l+1)M_{l+1}f_{13k-l}-
k_8\left(K_{13}^{-1}\right)^{n_{13}}f_{13k}+d_5\left(M_k+\left(K_{14}^{-1}\right)^{n_{14}}\sum_{l=0}^{k}M_lf_{14k-l}+\left(K_{13}^{-1}\right)^{n_{13}}\sum_{l=0}^{k}M_lf_{13k-l}\right)=0 \quad (49)
$$

$$
(k+1)R_{k+1}+\left(K_{16}^{-1}\right)^{n_{16}}\sum_{l=0}^{k}(l+1)R_{l+1}f_{16k-l}+\left(K_{15}^{-1}\right)^{n_{15}}\sum_{l=0}^{k}(l+1)R_{l+1}f_{13k-l}-k_9\left(K_{15}^{-1}\right)^{n_{15}}f_{15k}
+d_6\left(R_k+\left(K_{16}^{-1}\right)^{n_{16}}\sum_{l=0}^{k}R_lf_{16k-l}+\left(K_{15}^{-1}\right)^{n_{15}}\sum_{l=0}^{k}R_lf_{13k-l}\right)=0 \quad (50)
$$

Where

With transformed initial conditions given as:

$$
\begin{aligned}
S_0&=0\\
Y_0&=0\\
T_0&=0\\
P_0&=0\\
M_0&=0\\
R_0&=0
\end{aligned} \quad (51)
$$

Other conditions as a result of representation as also given as:

$$
\begin{aligned}
f_{2_0}&=\xi_2 & f_{4_0}&=\xi_4\\
f_{6_0}&=\xi_6 & f_{8_0}&=\xi_8\\
f_{9_0}&=\xi_9 & f_{10_0}&=\xi_{10}\\
f_{11_0}&=\xi_{11} & f_{12_0}&=\xi_{12}\\
f_{13_0}&=\xi_{13} & f_{14_0}&=\xi_{14}\\
f_{15_0}&=\xi_{15} & f_{16_0}&=\xi_{16}
\end{aligned} \quad (52)
$$

Performing iteration on equations (33–50) using equations (51–52) and applying the principle of DTM grouping of term by term solution, the following are obtained:

$$
\begin{aligned}
S(t)&=\sum_{k=0}^{N}S_kt^k & i&=1,2\\
T(t)&=\sum_{k=0}^{N}T_kt^k & i&=1,2\\
P(t)&=\sum_{k=0}^{N}P_kt^k & i&=1,2\\
M(t)&=\sum_{k=0}^{N}M_kt^k & i&=1,2\\
R(t)&=\sum_{k=0}^{N}R_kt^k & i&=1,2\\
Y(t)&=\sum_{k=0}^{N}Y_kt^k & i&=1,2
\end{aligned} \quad (53)
$$

Which in expanded form becomes:

$$
q(t)=q_0+q_1t+q_2t^2+\ldots \qquad where\ \ q\,f(S,T,P,M,R,Y) \quad (54)
$$

Equations (13) and (14) are the desired analytical solutions for deflection and rotation of the system. In order to capture deflection for large time history, after treatment technique is applied and the results are used to analyse the dynamic behaviour of the system in the present study.

RESULTS

In this study, a mathematical analysis of the mechanotransduction of mesenchymal stem cell fate decisions for biomaterials has been investigated. The governing

Making necessary substitution, the desired transient re-

$$S(t)=S_0+\begin{pmatrix}-k_1\left(\left(K_2^{-1}\right)^{n_2}\right)^2\xi_2^{\,2}-k_2\left(\left(K_4^{-1}\right)^{n_4}\right)^2\xi_4^{\,2}-\\ k_4\left(\left(K_8^{-1}\right)^{n_8}\right)^2\xi_8^{\,2}-2\left(K_2^{-1}\right)^{n_2}\left(\frac{X}{K_1}\right)^{n_1}k_1\xi_2-\\ 2\left(\frac{X}{K_3}\right)^{n_3}\left(K_4^{-1}\right)^{n_4}k_2\xi_4-2\left(K_6^{-1}\right)^{n_6}\left(\frac{X}{K_5}\right)^{n_5}\xi_6k_3-\\ 2\left(K_8^{-1}\right)^{n_8}\left(\frac{X}{K_7}\right)^{n_7}\xi_8k_4-k_1\left(\left(\frac{X}{K_1}\right)^{n_1}\right)^2-\\ k_2\left(\left(\frac{X}{K_3}\right)^{n_3}\right)^2-k_3\left(\left(\frac{X}{K_5}\right)^{n_5}\right)^2-k_4\left(\left(\frac{X}{K_7}\right)^{n_7}\right)^2+\\ \left(K_2^{-1}\right)^{n_2}k_1\xi_2+\left(K_4^{-1}\right)^{n_4}k_2\xi_4+\left(K_6^{-1}\right)^{n_6}\xi_6k_3+\\ \left(K_8^{-1}\right)^{n_8}\xi_8k_4+\left(\frac{X}{K_1}\right)^{n_1}k_1+k_3\left(\left(K_6^{-1}\right)^{n_6}\right)^2\xi_6^{\,2}-\\ \left(\frac{X}{K_3}\right)^{n_3}k_2+\left(\frac{X}{K_5}\right)^{n_5}k_3+\left(\frac{X}{K_7}\right)^{n_7}k_4\end{pmatrix}t+\ldots \tag{55}$$

$$T(t)=T_0+\left(\frac{k_6\left(K_9^{-1}\right)^{n_9}\xi_9}{\left(K_9^{-1}\right)^{n_9}\xi_9+\left(K_{10}^{-1}\right)^{n_{10}}\xi_{10}+1}\right)t+$$

$$\frac{-1/2k_6\left(K_9^{-1}\right)^{n_9}\xi_9}{(\Gamma)\begin{pmatrix}1+\left(\left(K_9^{-1}\right)^{n_9}\right)^2\xi_9^{\,2}+\\ 2\left(K_9^{-1}\right)^{n_9}\left(K_{10}^{-1}\right)^{n_{10}}\xi_{10}\xi_9+\\ \left(\left(K_{10}^{-1}\right)^{n_{10}}\right)^2\xi_{10}^{\,2}+\\ 2\left(K_9^{-1}\right)^{n_9}\xi_9+2\left(K_{10}^{-1}\right)^{n_{10}}\xi_{10}\end{pmatrix}}t^2$$

$$\begin{pmatrix}\left(\left(K_8^{-1}\right)^{n_8}\right)^2\left(K_{10}^{-1}\right)^{n_{10}}k_4n_9\xi_{10}\xi_8^{\,2}-\left(K_2^{-1}\right)^{n_2}\left(K_{10}^{-1}\right)^{n_{10}}k_1n_9\xi_{10}\xi_2-\\ \left(K_4^{-1}\right)^{n_4}\left(K_{10}^{-1}\right)^{n_{10}}k_2n_9\xi_{10}\xi_4-\left(K_6^{-1}\right)^{n_6}\left(K_{10}^{-1}\right)^{n_{10}}k_3n_9\xi_{10}\xi_6-\\ \left(K_8^{-1}\right)^{n_8}\left(K_{10}^{-1}\right)^{n_{10}}k_4n_9\xi_{10}\xi_8+\left(\left(K_2^{-1}\right)^{n_2}\right)^2\left(K_{10}^{-1}\right)^{n_{10}}k_1n_9\xi_{10}\xi_2^{\,2}+\\ \left(\left(K_4^{-1}\right)^{n_4}\right)^2\left(K_{10}^{-1}\right)^{n_{10}}k_2n_9\xi_{10}\xi_4^{\,2}+\left(\left(K_6^{-1}\right)^{n_6}\right)^2\left(K_{10}^{-1}\right)^{n_{10}}k_3n_9\xi_{10}\xi_6^{\,2}+\\ 2\left(\frac{X}{K_1}\right)^{n_1}\left(K_2^{-1}\right)^{n_2}\left(K_{10}^{-1}\right)^{n_{10}}k_1n_9\xi_{10}\xi_2+2\left(\frac{X}{K_3}\right)^{n_3}\left(K_4^{-1}\right)^{n_4}\left(K_{10}^{-1}\right)^{n_{10}}k_2n_9\xi_{10}\xi_4\\ +2\left(\frac{X}{K_5}\right)^{n_5}\left(K_6^{-1}\right)^{n_6}\left(K_{10}^{-1}\right)^{n_{10}}k_3n_9\xi_{10}\xi_6+2\left(\frac{X}{K_7}\right)^{n_7}\left(K_8^{-1}\right)^{n_8}\left(K_{10}^{-1}\right)^{n_{10}}k_4n_9\xi_{10}\xi_8+\\ \left(\left(K_2^{-1}\right)^{n_2}\right)^2k_1n_9\xi_2^{\,2}+\left(\left(K_4^{-1}\right)^{n_4}\right)^2k_2n_9\xi_4^{\,2}+\left(\left(K_6^{-1}\right)^{n_6}\right)^2k_3n_9\xi_6^{\,2}+\\ \left(\left(K_8^{-1}\right)^{n_8}\right)^2k_4n_9\xi_8^{\,2}+(\Gamma)\left(K_9^{-1}\right)^{n_9}d_3\xi_9+(\Gamma)\left(K_{10}^{-1}\right)^{n_{10}}d_3\xi_{10}-\left(K_2^{-1}\right)^{n_2}k_1n_9\xi_2-\\ \left(K_4^{-1}\right)^{n_4}k_2n_9\xi_4-\left(K_6^{-1}\right)^{n_6}k_3n_9\xi_6-\left(K_8^{-1}\right)^{n_8}k_4n_9\xi_8+(\Gamma)d_3+\left(\left(\frac{X}{K_5}\right)^{n_5}\right)^2k_3n_9+\\ \left(\frac{X}{K_1}\right)^{n_1}k_1n_9-\left(\frac{X}{K_1}\right)^{n_1}k_1n_9-\left(\frac{X}{K_7}\right)^{n_7}k_4n_9-\left(\frac{X}{K_3}\right)^{n_3}k_3n_9-\left(\frac{X}{K_3}\right)^{n_3}k_2n_9+\\ \left(\frac{X}{K_3}\right)^{n_3}k_2n_9+\left(\left(\frac{X}{K_7}\right)^{n_7}\right)^2k_4n_9+2\left(\frac{X}{K_7}\right)^{n_7}\left(K_8^{-1}\right)^{n_8}k_4n_9\xi_8-\\ \left(\frac{X}{K_7}\right)^{n_7}\left(K_{10}^{-1}\right)^{n_{10}}k_4n_9\xi_{10}+\left(\left(\frac{X}{K_1}\right)^{n_1}\right)^2\left(K_{10}^{-1}\right)^{n_{10}}k_1n_9\xi_{10}+\\ \left(\left(\frac{X}{K_3}\right)^{n_3}\right)^2\left(K_{10}^{-1}\right)^{n_{10}}k_2n_9\xi_{10}+\left(\left(\frac{X}{K_5}\right)^{n_5}\right)^2\left(K_{10}^{-1}\right)^{n_{10}}k_3n_9\xi_{10}+\\ \left(\left(\frac{X}{K_7}\right)^{n_7}\right)^2\left(K_{10}^{-1}\right)^{n_{10}}k_4n_9\xi_{10}+2\left(\frac{X}{K_1}\right)^{n_1}\left(K_2^{-1}\right)^{n_2}k_1n_9\xi_2-\\ \left(\frac{X}{K_1}\right)^{n_1}\left(K_{10}^{-1}\right)^{n_{10}}k_1n_9\xi_{10}+2\left(\frac{X}{K_3}\right)^{n_3}\left(K_4^{-1}\right)^{n_4}k_2n_9\xi_4-\\ \left(\frac{X}{K_3}\right)^{n_3}\left(K_{10}^{-1}\right)^{n_{10}}k_2n_9\xi_{10}+2\left(\frac{X}{K_5}\right)^{n_5}\left(K_6^{-1}\right)^{n_6}k_3n_9\xi_6-\left(\frac{X}{K_5}\right)^{n_5}\left(K_{10}^{-1}\right)^{n_{10}}k_3n_9\xi_{10}\end{pmatrix} \tag{56}$$

$$P(t)=P_0+\frac{k_7\left(K_{11}^{-1}\right)^{n_{11}}\xi_{11}t}{\left(K_{11}^{-1}\right)^{n_{11}}\xi_{11}+\left(K_{12}^{-1}\right)^{n_{12}}\xi_{12}+1}+\ldots \tag{57}$$

$$M(t)=M_0+\frac{k_8\left(K_{13}^{-1}\right)^{n_{13}}\xi_{13}t}{\left(K_{14}^{-1}\right)^{n_{14}}\xi_{14}+\left(K_{13}^{-1}\right)^{n_{13}}\xi_{13}+1}+\ldots \tag{58}$$

$$R(t)=R_0+\frac{k_9\left(K_{15}^{-1}\right)^{n_{15}}\xi_{15}t}{\left(K_{16}^{-1}\right)^{n_{16}}\xi_{16}+\left(K_{15}^{-1}\right)^{n_{13}}\xi_{13}+1}+\ldots \tag{59}$$

$$Y(t)=Y_0-1/2k_5\begin{pmatrix}k_1\left(\left(K_2^{-1}\right)^{n_2}\right)^2\xi_2^{\,2}+k_2\left(\left(K_4^{-1}\right)^{n_4}\right)^2\xi_4^{\,2}+k_3\left(\left(K_6^{-1}\right)^{n_6}\right)^2\xi_6^{\,2}+\\ k_4\left(\left(K_8^{-1}\right)^{n_8}\right)^2\xi_8^{\,2}+2\left(K_2^{-1}\right)^{n_2}\left(\frac{X}{K_1}\right)^{n_1}k_1\xi_2+\\ 2\left(\frac{X}{K_3}\right)^{n_3}\left(K_4^{-1}\right)^{n_4}k_2\xi_4+2\left(K_6^{-1}\right)^{n_6}\left(\frac{X}{K_5}\right)^{n_5}\xi_6k_3+\\ 2\left(K_8^{-1}\right)^{n_8}\left(\frac{X}{K_7}\right)^{n_7}\xi_8k_4+k_1\left(\left(\frac{X}{K_1}\right)^{n_1}\right)^2+-\left(\frac{X}{K_7}\right)^{n_7}k_4\\ k_2\left(\left(\frac{X}{K_3}\right)^{n_3}\right)^2+k_3\left(\left(\frac{X}{K_5}\right)^{n_5}\right)^2+k_4\left(\left(\frac{X}{K_7}\right)^{n_7}\right)^2-\\ \left(K_2^{-1}\right)^{n_2}k_1\xi_2-\left(K_4^{-1}\right)^{n_4}k_2\xi_4-\left(K_6^{-1}\right)^{n_6}\xi_6k_3-\\ \left(K_8^{-1}\right)^{n_8}\xi_8k_4-\left(\frac{X}{K_1}\right)^{n_1}k_1-\left(\frac{X}{K_3}\right)^{n_3}k_2-\left(\frac{X}{K_5}\right)^{n_5}k_3\end{pmatrix}t^2+\ldots \tag{60}$$

equation, which is a set of coupled nonlinear ordinary differential equation was solved analytically by using the Differential Transform Method (DTM). The results are validated using the Fourth Order Runge Kutta method numerical solution and presented in Table 2. The error analysis carried out showed that an accepted error of less than 3% was observed in the differences of the solutions between the results obtained from the DTM and the numerical method.

The obtained results for varying parameters are here presented. The stiffness relative levels and the effective stiffness adhesion area are represented with *X* and *S*, respectively. And *Y, T, P, M,* and *R* represent the relative concentrations of *YAP/ TAZ, TUBB3, PPARG, MYOD1,* and *RUNX2*. The effects of the stiffness level on relative concentration rates are shown in Figures 3–6. *Y* also behaves as an upstream factor for the cell differentiation genes. This makes it possible for the inhibition of *T* to be attenuated by *Y* depletion, whereas that the factor *P* binding to *T* results in inhibition of transcription from the promoter components. T is the enhancer function for difference resolution in *M* myogenic differentiation. Finally, *R* is bonded to *T* and causes osteocalcin expression, hence enhancing osteogenic differentiation.

Table 2: Validation of DTM with Numerical Runge-Kutta

Time	*Concentration rate of Y*			*Concentration rate of T*		
(t)	Numerical	DTM	Residual	Numerical	DTM	Residual
0.00	0.0000000	0.0000000	0.0000000	0.0000000	0.0000000	0.0000000
0.50	5.9171396	5.9171349	0.0000047	0.3819499	0.3819497	0.0000001
1.00	17.3335042	17.3334904	0.0000137	0.2316653	0.2316652	0.0000001
1.50	29.0054579	29.0054350	0.0000230	0.1405121	0.1405120	0.0000001
2.00	38.9644096	38.9643788	0.0000308	0.0852249	0.0852248	0.0000000
2.50	46.7513598	46.7513229	0.0000369	0.0516915	0.0516915	0.0000000
3.00	52.5337552	52.5337153	0.0000399	0.0313525	0.0313525	0.0000000
3.50	56.6836004	56.6835623	0.0000382	0.0190162	0.0190162	0.0000000
4.00	59.5904839	59.5904505	0.0000333	0.0115339	0.0115339	0.0000000
4.50	61.5901135	61.5900860	0.0000275	0.0069957	0.0069957	0.0000000
5.00	62.9464244	62.9464023	0.0000221	0.0042431	0.0042431	0.0000000
5.50	63.8560997	63.8560821	0.0000176	0.0025736	0.0025736	0.0000000
6.00	64.4606381	64.4606239	0.0000141	0.0015609	0.0015609	0.0000000
6.50	64.8593314	64.8593199	0.0000116	0.0009468	0.0009468	0.0000000
7.00	65.1205764	65.1205667	0.0000097	0.0005742	0.0005742	0.0000000
7.50	65.2908114	65.2908029	0.0000084	0.0003483	0.0003483	0.0000000
8.00	65.4012110	65.4012035	0.0000075	0.0002112	0.0002112	0.0000000
8.50	65.4725071	65.4725002	0.0000069	0.0001281	0.0001281	0.0000000
9.00	65.5183801	65.5183736	0.0000065	0.0000777	0.0000777	0.0000000
9.50	65.5477988	65.5477926	0.0000062	0.0000471	0.0000471	0.0000000
10.00	65.5666101	65.5666041	0.0000060	0.0000286	0.0000286	0.0000000
10.50	65.5786069	65.5786010	0.0000059	0.0000173	0.0000173	0.0000000
11.00	65.5862382	65.5862324	0.0000058	0.0000105	0.0000105	0.0000000
11.50	65.5910833	65.5910775	0.0000058	0.0000064	0.0000064	0.0000000
12.00	65.5941537	65.5941480	0.0000058	0.0000039	0.0000039	0.0000000
12.50	65.5960938	65.5960880	0.0000057	0.0000023	0.0000023	0.0000000
13.00	65.5973207	65.5973150	0.0000057	0.0000014	0.0000014	0.0000000
13.50	65.5980920	65.5980863	0.0000057	0.0000009	0.0000009	0.0000000
14.00	65.5985794	65.5985737	0.0000057	0.0000005	0.0000005	0.0000000
14.50	65.5988845	65.5988788	0.0000057	0.0000003	0.0000003	0.0000000
15.00	65.5990762	65.5990705	0.0000057	0.0000002	0.0000002	0.0000000

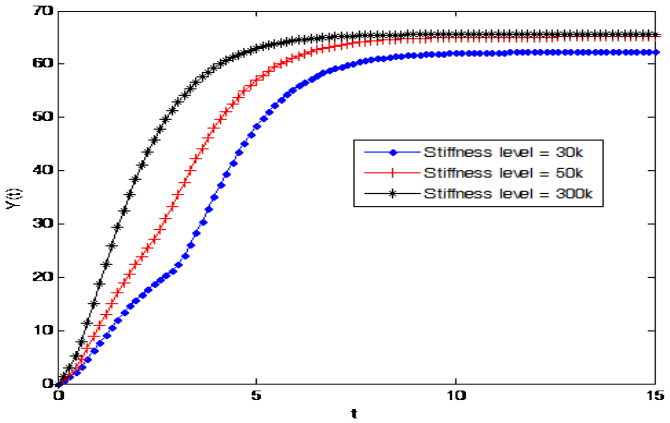

Fig. 3: Impact of Stiffness Level on Y (t) *YAP/TAZ* (Transcriptional Coactivator).

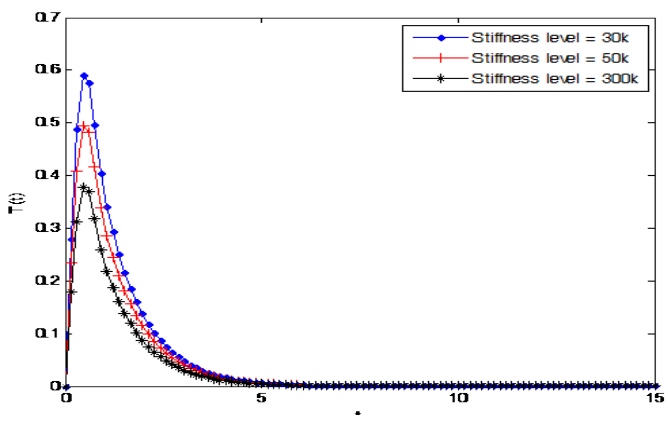

Fig. 4: Impact of Stiffness Level on T (t) *TUBB3* (Gene Encoded Tubulin Beta-3chain).

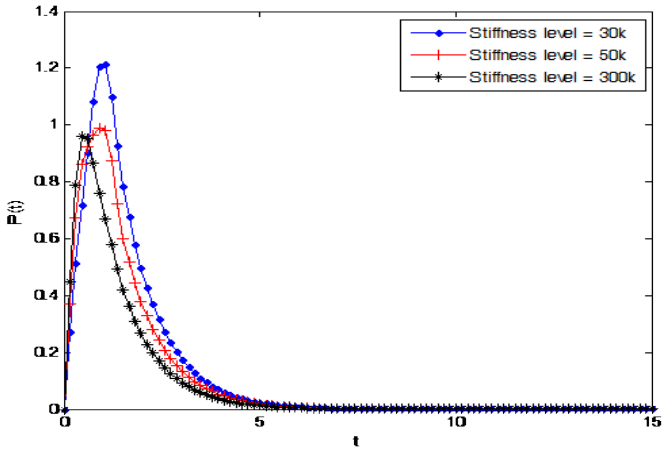

Fig. 5: Impact of Stiffness Level on P (t) *PPARG* (Peroxisome Proliferator-Activated Receptor Gamma).

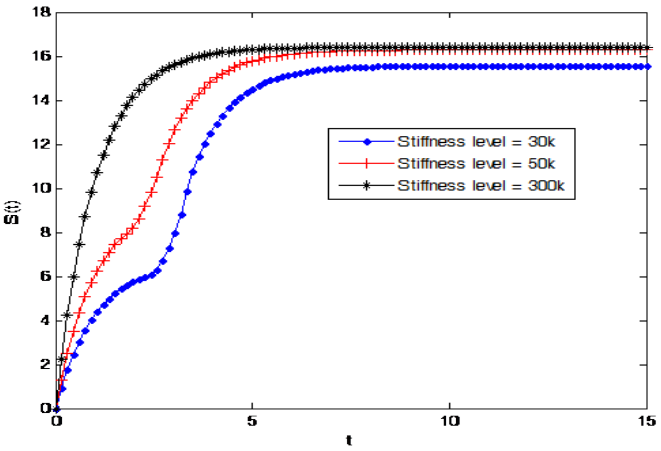

Fig. 7: Impact of Large Stiffness Level k1 on S (t) (Effective Stiffness Adhesion Area).

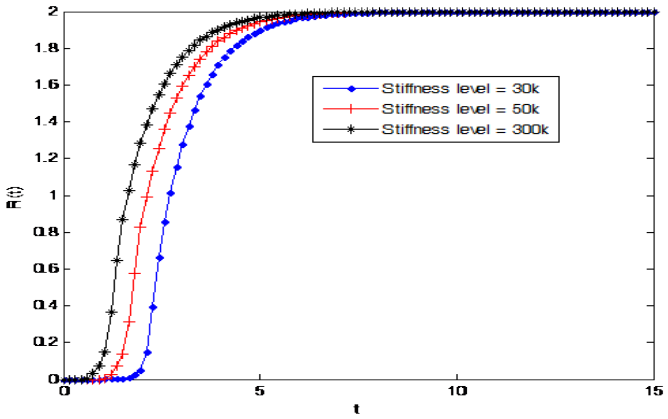

Fig. 6: Impact of Stiffness Level on R (t) *RUNX2* (Runt-Related Transcription Factor 2).

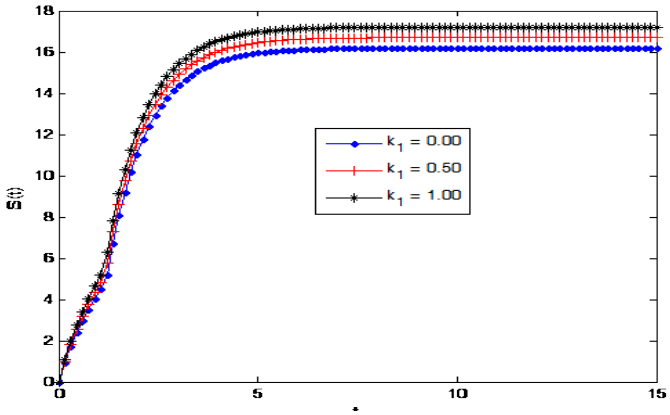

Fig. 8: Impact of Low Stiffness Level k1 on S (t) (Effective Stiffness Adhesion Area).

The effects of large stiffness level (30k–300k) k_1 on effective stiffness adhesion area are shown in Figure 7. From the results, it is observed that when the system's stiffness level is low, the effective stiffness adhesion area reduces. However, at very large stiffness level, the curve becomes asymptotic and further increase in this value possesses negligible impact on the effective stiffness adhesion area. The effect of low stiffness level (0k-1.0k) k_1 on effective stiffness adhesion area is shown in Figure 8. The plot shows that an increase in the parameter shows a negligible impact on the effective stiffness adhesion area for short period. However, as the transient process is considered over a wider range of the independent variable, an increase in low stiffness level k_1 causes a corresponding increase in effective stiffness adhesion area. This parameter may be used to annul the reducing impacts witnessed in the transient behaviour of *P* and *T.*

The effect of degradation rate of the corresponding gene factor d_1 on effective stiffness adhesion area is shown in Figure 9. The plot shows that an increase in the parameter shows a negligible impact on the effective stiffness adhesion area at the initial state of response. However, as the transient process is considered over a wider time range, an increase in degradation rate factor d_1 causes a decrease in effective stiffness adhesion area. This parameter may be used to inhibit the transient responses of *Y* and *R.*

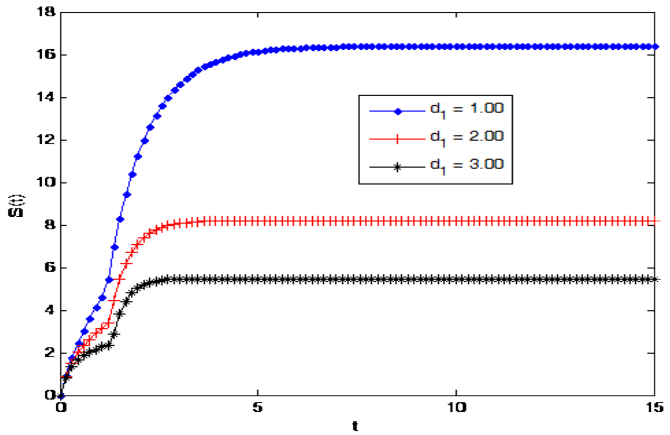

Fig. 9: Impact of Degradation Rate of the Corresponding Gene Factor d1 on S (t).

DISCUSSION

The fate of mesenchymal stem cell can be regulated by mechanical dosing and past mechanical dosing or memory also affects the fate of the stem cell, particularly when there is stiffness in the initial substrate. However it is difficult to investigate the effects of mechanical memory by experiments over a wide range of cultured conditions. Hence, a developed mathematical model was analytically investigated. It allows such investigations to be carried out, and striking results to be predicted as observed in the study. In the investigated dynamic model, the behaviours of several parameters were also observed as they were increased or decreased. The stiffness parameters of the dynamic model at high and low levels have significant effects on the effective stiffness adhesion area. Similarly, the degradation rates of the corresponding gene factor also have significant effects on the effective stiffness adhesion area. These parameters are very important in determining the fate of mesenchymal stem cell induced by mechanical stimuli for cell-differentiation or cell growth. Consequently, they are of great importance in the dynamical analysis of the mechano-transduction of mesenchymal stem cell and the analytical investigation can be applied in developing new techniques for controlling the fate of mesenchymal stem cell's transplantation and designs of new biomaterials.

It was observed from all the obtained results that the applied analytical method in this study provides a better understanding of the physical quantities in the dynamical model of the mechanotransduction of mesenchymal stem cell. This would not have been achieved by applying the conventional numerical schemes used for nonlinear governing models. Thus the analytical method was applied to obtain the desired solutions. These solutions were compared with past simulated results obtained by Peng *et al.* (7) and good agreement was established between the two results. The direct relationship of the parameters in the model and their physical meaning is also shown by the applied method for the governing model. For instance, at low values of the system's high stiffness (30k–300k), the effective stiffness adhesion area reduces, and at very large stiffness level, the curve becomes asymptotic, and when it is further increased, it has a negligible impact on the effective stiffness adhesion area. And it is observed that an increase in the low stiffness k_1 causes a corresponding increase in effective stiffness adhesion area, while an increase in degradation rate factor d_1 causes a decrease in effective stiffness adhesion area. The applied analytical method made these observations noticeable. The method also provides a platform for predicting new memory regions that can influence MSCs fate decisions because of the direct relationship among the parameters of the governing model.

CONCLUSION

In this study, the analytical investigation of the mechanotransduction of mesenchymal stem cell fate decisions for biomaterials using differential transform method has been presented. The nonlinear dynamical model of the mechanotransduction of mesenchymal stem cell that is capable of describing the cell fate behaviour during mechanical stimuli directed cell-differentiation was developed. The developed model was solved by applying the Differential Transform Method (DTM) and verified using the forth order Runge-Kutta numerical method (RK4). The obtained results were compared with the results obtained in earlier studies. Good agreements were reached in all the results. The effects of systems' large (30k–300k) and low (0k–1.0k) stiffness levels, k_1 and degradation rate of the corresponding gene factor d_1 on effective stiffness adhesion area were investigated. At low values of the system's high stiffness (30k–300k), the effective stiffness adhesion area reduces, and at very large stiffness level, the curve becomes asymptotic, but when it is further increased, it has a negligible impact on the effective stiffness adhesion area. It is also observed that at low values of the system's low stiffness (0k–1.0k), the low stiffness k_1 and degradation rate of the corresponding gene factor d_1 shows a negligible impact on the effective stiffness adhesion area at the initial state of response, while an increase in the low stiffness k_1 causes a corresponding increase in effective stiffness adhesion area, but an increase in degradation rate factor d_1 causes a decrease in effective stiffness adhesion area. Finally from the study, new memory regions that can influence MSCs fate decisions can be predicted, and the obtained results from the dynamical analysis can be applied in developing new and better techniques in controlling the fate of MSCs transplantation and designs of new biomaterials.

ACKNOWLEDGMENT

We acknowledge the provision of computer systems for simulation of results by Energy Research Laboratory, Faculty of Engineering, University of Lagos, Nigeria.

CONFLICT OF INTEREST

The authors of this paper have declared that there is no conflict of interest in this study with respect to the authorship and the publication of the research work.

REFERENCES

1. Anderson HJ, Sahoo JK, Ulijn RV, Dalby MJ. Mesenchymal stem cell fate: applying biomaterials for control of stem cell behavior. *Front Bioeng Biotechnol.* 2016; **4(38):** 1–14.
2. Murphy V, Atala A. Organ engineering – combining stem cells biomaterials and bioreactors to produce bioengineererd organs for transplantation. *Bioessays.* 2013; **35(3):** 163–172.
3. Hubbell JA. Materials as morphogenetic guides in tissue engineering. *Curr Opin Biotechnology.* 2003; **14:** 551–558.
4. Guilak F, Cohen DM, Estes BT, Gimble JM, Liedtke W, Chen CS. Control of stem cell fate by physical interactions with the extracellular matrix. *Cell Stem Cell.* 2009; **5:** 17–26.
5. Burridge K, Chrzanowska-Wodnicka M. Focal adhesions, contractility, and signaling. *Annu Rev Cell Dev Biol.* 1996; **12:** 463–518.

6. Sun M, Spill F, Zaman MH. A computational model of YAP/TAZ mechanosensing. *Biophys J.* 2016; **110(11):** 2540–2550.
7. Peng T, Liu L, MacLean AL, Wong CW, Zhao W, Nie Q. A mathematical model of mechanotransduction reveals how mechanical memory regulates mesenchymal stem cell fate decisions. *BMC Syst Biol.* 2017; **11(1):** 55. doi: 10.1186/s12918-017-0429-x.
8. Diba M, Spaans S, Ning Ke, Ippel B. Self-healing biomaterials: from molecular concepts to clinical applications. *Adv Mater Interfaces.* 2018; **5(17):** 1–21.
9. Lotfi M, Nejib M, Naceur M. *Cell adhesion to biomaterials: Concept of biocompability*. In: Advances in Biomaterials Science and Biomedical Applications. Rosario Pignatello (Eds.). March 2013, https://doi.org/10.5772/53542.
10. Sthijns MM, LaPointe VLS, van Blitterswijk CA. Building complex life through Self-Organization. *Tissue Eng Part A.* 2019; **25(19–0):** 1341–1346.
11. Tong Z, Jia X. Biomaterials-based strategies for the engineering of mechanically active soft tissues. *MRS Commun.* 2012; **2(2):** 31–39.
12. Trappmann B, Gautrot JE, Connelly JT, Strange DG, Li Y, Oyen ML. Extracellular-matrix tethering regulates stem-cell fate. *Nature Mater.* 2012; **11:** 642–649.
13. Arnold M, Hirschfeld-Warneken VC, Lohmüller T, Heil P, Blümmel J. Induction of cell polarization and migration by a gradient of nanoscale variations in adhesive ligand spacing. *Nano Letters.* 2008; **8:** 2063–2069.
14. Lindvall O, Kokaia Z, Martinez-Serano A. Stem cell therapy for human neurodegenerative disorders – how to make it work. *Nat Med.* 2004; **10:** S42–S50.
15. Lutolf MP, Gilbert PM, Blau HM. Designing materials to direct stem-cells fate. *Nature.* 2009; **462**(7272): 433–441.
16. Yim EK, Reano RM, Pang SW, Yee AF, Che CS, Leon KW. Nanopattern-induced changes in morphology and motility of smooth muscle cells. *Biomaterials.* 2005; **26(26):** 5405–5413.
17. Geiger B, Bershadsky A, Pankov R, Yamada KM. Transmembrane crosstalk between the extracellular matrix-cytoskeleton crosstalk. *Nat Rev Mol Cell Biol.* 2001; **2(11):** 793–805.
18. Oreffo RO, Cooper C, Mason C, Clements M. Mesenchymal stem cells: lineage, plasticity, and skeletal therapeutic potential. *Stem Cell Rev.* 2005; **1(2):** 169–178.
19. Dalby MJ, Gadegaard N, Oreffo RO. Harnessing nano topography and integrin-matrix interactions to influence stem cell fate. *Nat Mater.* 2014; **13:** 558–569.
20. Hench LL, Polak JM. Third-generation biomedical materials. *Science.* 2002; **295(5557):** 1014–1017.
21. Engler AJ, Sen S, Sweeney HL, Discher DE. Matrix elasticity directs stem cell lineage specification. *Cell.* 2006; **126(4):** 677–689.
22. Ingalls B. *Mathematical Modelling in Systems Biology: An Introduction.* The MIT Press, 2013.
23. Zhou JK. *Differential Transform Method and Its Applications for Electrical Circuits.* Huazhong University Press, Wuhan, China, 1986.
24. Acharya N, Das K, Kundu PK. The squeezing flow of Cu-water and Cu-kerosene nanofluids between two parallel plates. *Alex Eng J.* 2016; **55(2):** 1177–1186.
25. Hatami M, Jing D. Differential transformation method for newtonian and non-newtonian nanofluids flow analysis: compared to numerical solution. *Alex Eng J.* 2016; **55(2):** 731–739.
26. Mosayebidorcheh S, Farzinpoor M, Ganji DD. Transient thermal analysis of longitudinal fins with internal heat generation considering temperature-dependent properties and different fin profiles. *Energy Convers Manag.* 2014; **86:** 365–370.
27. Adeleye OA, Ipinnimo O, Yinusa A, Otobo EP. Dynamic analysis of the biomechanical model of head load impact using differential transform method. *J Appl Comput Mech.* 2020; **6(4):** 893–907.
28. Ramesh RT. A comparison between the differential transform method and homotopy perturbation method for a system of non linear chemistry problems. *Indian J Appl Res.* 2016; **6(2):** 171–180.
29. Cakir M, Arslan D. The adomian decomposition method and the differential transform method for numerical solution of multi-pantograph delay differential equations. *Appl Math Lett.* 2015; **6(8):** 1332–1343.
30. Nazari D, Shahmorad S. Application of the fractional differential transform method to fractional-order integro-differential equations with nonlocal boundary conditions. *J Comput Appl Math.* 2010; **234(3):** 883–891.
31. Nourazar S, Mirzabeigy A. Approximate solution for nonlinear Duffing oscillator with damping effect using the modified differential transform method. *Sci. Iran.* 2013; **20(2):** 364–368.